Australian Journal of Basic and Applied Sciences, 4(8): 2280-2291, 2010
ISSN 1991-8178

Control Schemes for Input Tracking and Anti-sway Control of a Gantry Crane

M. A. Ahmad, A.N.K. Nasir, R.M.T. Raja Ismail, M.S. Ramli

Control and Instrumentation Research Group Faculty of Electrical and Electronics Engineering, Universiti Malaysia Pahang, Malaysia.

Abstract: This paper presents investigations into the development of hybrid control schemes for input tracking and anti-sway control of a gantry crane system. A nonlinear overhead gantry crane system is considered and the dynamic model of the system is derived using the Euler-Lagrange formulation. To study the effectiveness of the controllers, an LQR control is developed for cart position control of a gantry crane. This is then extended to incorporate input shaper control schemes for anti-sway control of the system. The positive and new modified specified negative amplitude (SNA) input shapers are then designed based on the properties of the system for control of system sway. The new SNA is proposed to improve the robustness capability while increasing the speed of the system response. Simulation results of the response of the gantry crane with the controllers are presented in time and frequency domains. The performances of the of the hybrid control schemes are examined in terms of input tracking capability, level of sway reduction and robustness to parameters uncertainty. A comparative assessment of the hybrid controllers to the system performance is presented and discussed.

Key words: Gantry crane, anti-sway control, input shaping, LQR controller.

INTRODUCTION

The main purpose of controlling a gantry crane is transporting the load as fast as possible without causing any excessive sway at the final position. However, most of the common gantry crane results in a sway motion when payload is suddenly stopped after a fast motion (Omar, 2003). The sway motion can be reduced but will be time consuming. Moreover, the gantry crane needs a skilful operator to control manually based on his or her experiences to stop the sway immediately at the right position. The failure of controlling crane also might cause accident and may harm people and the surrounding.

The requirement of precise cart position control of gantry crane implies that residual sway of the system should be zero or near zero. Over the years, investigations have been carried out to devise efficient approaches to reduce the sway of gantry crane. The considered sway control schemes can be divided into two main categories: feed-forward control and feedback control techniques. Feed-forward techniques for sway suppression involve developing the control input through consideration of the physical and swaying properties of the system, so that system sways at dominant response modes are reduced. This method does not require additional sensors or actuators and does not account for changes in the system once the input is developed. On the other hand, feedback-control techniques use measurement and estimations of the system states to reduce sways. Feedback controllers can be designed to be robust to parameter uncertainty. For gantry crane, feed-forward and feedback control techniques are used for sway suppression and cart position control respectively. An acceptable system performance without sway that accounts for system changes can be achieved by developing a hybrid controller consisting of both control techniques. Thus, with a properly designed feed-forward controller, the complexity of the required feedback controller can be reduced.

Various attempts in controlling gantry cranes system based on feed-forward control schemes were proposed. For example, open loop time optimal strategies were applied to the crane by many researchers such as discussed in (Manson,1992; Auernig and Troger, 1987). They came out with poor results because feed-forward strategy is sensitive to the system parameters (e.g. rope length) and could not compensate for wind disturbances. Another feed-forward control strategy is input shaping (Karnopp *et al.,* 1992; Teo *et al.,* 1998; Singhose *et al.,* 1997). Input shaping is implemented in real time by convolving the command signal with an

Corresponding Author: Mohd Ashraf Ahmad, Faculty of Electrical and Electronics Engineering Universiti Malaysia Pahang Pekan, 26600, Pahang, Malaysia.
Tel: 609-4242070; Fax: 609-4242032
Email: mashraf@ump.edu.my

impulse sequence. The process has the effect of placing zeros at the locations of the flexible poles of the original system. An IIR filtering technique related to input shaping has been proposed for controlling suspended payloads (Feddema, 1993). Input shaping has been shown to be effective for controlling oscillation of gantry cranes when the load does not undergo hoisting (Noakes and Jansen, 1992; Singer *et al.,* 1997). Experimental results also indicate that shaped commands can be of benefit when the load is hoisted during the motion (Kress *et al.,* 1994).

Investigations have shown that with the input shaping technique, a system response with delay is obtained. To reduce the delay and thus increase the speed of the response, negative amplitude input shapers have been introduced and investigated in vibration control. By allowing the shaper to contain negative impulses, the shaper duration can be shortened, while satisfying the same robustness constraint. A significant number of negative shapers for vibration control have also been proposed. These include negative unity-magnitude (UM) shaper, specified-negative-amplitude (SNA) shaper, negative zero-vibration (ZV) shaper, negative zero-vibration-derivative (ZVD) shaper and negative zero-vibration-derivative-derivative (ZVDD) shaper (Singhose *et al.,* 1994; Singhose and Mills, 1999; Mohamed *et al.,* 2006). Comparisons of positive and negative input shapers for vibration control of a single-link flexible manipulator have also been reported (Mohamed *et al.,* 2006).

On the other hand, feedback control which is well known to be less sensitive to disturbances and parameter variations (Belanger, 1995) is also adopted for controlling the gantry crane system. Recent work on gantry crane control system was presented by (Omar, 2003). The author had proposed proportional-derivative PD controllers for both position and anti-sway controls. Furthermore, a fuzzy-based intelligent gantry crane system has been proposed (Wahyudi and Jalani, 2005). The proposed fuzzy logic controllers consist of position as well as anti-sway controllers. However, most of the feedback control system proposed needs sensors for measuring the cart position as well as the load sway angle. In addition, designing the sway angle measurement of the real gantry crane system, in particular, is not an easy task since there is a hoisting mechanism.

This paper presents investigations into the development of hybrid control schemes for input tracking and anti-sway control of a gantry crane system. A nonlinear overhead gantry crane system is considered and the dynamic model of the system is derived using the Euler-Lagrange formulation. Hybrid control schemes based on feed-forward with collocated feedback controllers are investigated. In this work, feed-forward control based on input shaping with positive zero-sway-derivative-derivative (ZSDD) input shapers and new modified SNA zero-sway-derivative-derivative (ZSDD) input shapers are considered. A new modified shaper from the previous SNA input shapers (Mohamed *et al.,* 2006) is proposed where more negative impulses are added to improve the robustness of the controller while increasing the speed of the system response. To demonstrate the effectiveness of the proposed control schemes, an LQR controller is developed for control of cart motion of the gantry crane. This is then extended to incorporate the proposed input shapers for control of sway of hoisting rope. Simulation exercises are performed within the gantry crane simulation environment. Performances of the developed controllers are examined in terms of input tracking capability, level of sway reduction and robustness to errors in sway frequency. In this case, the robustness of the hybrid control schemes is assessed with up to 30% error tolerance in sway frequencies. Simulation results in time and frequency domains of the response of the gantry crane to the unshaped input and shaped inputs with positive and modified SNA input shapers are presented. Moreover, a comparative assessment of the effectiveness of the hybrid controllers with positive and negative input shapers in suppressing sway and maintaining the input tracking capability of the gantry crane is discussed.

The Gantry Crane System:

The two-dimensional gantry crane system with its payload considered in this work is shown in Figure 1, where x is the horizontal position of the cart, l is the length of the rope, θ is the sway angle of the rope, M and m is the mass of the cart and payload respectively. In this simulation, the cart and payload can be considered as point masses and are assumed to move in two-dimensional, x-y plane. The tension force that may cause the hoisting rope elongate is also ignored. In this study the length of the cart, l = 1.00 m, M = 2.49 kg, m = 1.00 kg and g = 9.81 m/s^2 is considered.

Modelling of the Gantry Crane:

This section provides a brief description on the modelling of the gantry crane system, as a basis of a simulation environment for development and assessment of the input shaping control techniques. The Euler-Lagrange formulation is considered in characterizing the dynamic behaviour of the crane system incorporating payload.

Considering the motion of the gantry crane system on a two-dimensional plane, the kinetic energy of the system can thus be formulated as

$$T = \frac{1}{2}M\dot{x}^2 + \frac{1}{2}m(\dot{x}^2 + \dot{l}^2 + l^2\dot{\theta}^2 + 2\dot{x}\dot{l}\sin\theta + 2\dot{x}l\dot{\theta}\cos\theta) \tag{1}$$

The potential energy of the beam can be formulated as

$$U = -mgl\cos\theta \tag{2}$$

To obtain a closed-form dynamic model of the gantry crane, the energy expressions in (1) and (2) are used to formulate the Lagrangian *L=T-U*. Let the generalized forces corresponding to the generalized displacements $\overline{q} = \{x, \theta\}$ be $\overline{F} = \{F_x, 0\}$. Using Lagrangian's equation

$$\frac{d}{dt}\left(\frac{\partial L}{\partial \dot{q}_j}\right) - \frac{\partial L}{\partial q_j} = F_j \qquad j = 1, 2 \tag{3}$$

the equation of motion is obtained as below,

$$F_x = (M+m)\ddot{x} + ml(\ddot{\theta}\cos\theta - \dot{\theta}^2\sin\theta) + 2m\dot{l}\dot{\theta}\cos\theta + m\ddot{l}\sin\theta \tag{4}$$

$$l\ddot{\theta} + 2\dot{l}\dot{\theta} + \ddot{x}\cos\theta + g\sin\theta = 0 \tag{5}$$

In order to develop an LQR control scheme, a linear model of gantry crane system is required. The linear model of the uncontrolled system can be represented in a state-space form as shown in equation (6) by assuming the change of rope and sway angle are very small.

$$\dot{x} = \mathbf{A}x + \mathbf{B}u$$
$$y = \mathbf{C}x \tag{6}$$

with the vector $x = \begin{bmatrix} x & \theta & \dot{x} & \dot{\theta} \end{bmatrix}^T$ and the matrices A and B are given by

$$\mathbf{A} = \begin{bmatrix} 0 & 0 & 1 & 0 \\ 0 & 0 & 0 & 1 \\ 0 & \frac{mg}{M} & 0 & 0 \\ 0 & -\frac{(M+m)g}{Ml} & 0 & 0 \end{bmatrix}, \quad \mathbf{B} = \begin{bmatrix} 0 \\ 0 \\ \frac{1}{M} \\ -\frac{1}{Ml} \end{bmatrix}, \quad \mathbf{C} = \begin{bmatrix} 1 & 0 & 0 & 0 \end{bmatrix}, \quad \mathbf{D} = \begin{bmatrix} 0 \end{bmatrix} \tag{7}$$

Lqr Control Scheme:

A more common approach in the control of manipulator systems involves the utilization linear quadratic regulator (LQR) design (Ogata, 1997). Such an approach is adopted at this stage of the investigation here. In order to design the LQR controller a linear state-space model of the gantry crane system was obtained by linearising the equations of motion of the system. For a LTI system

$$\dot{x} = \mathbf{A}x + \mathbf{B}u \tag{8}$$

the technique involves choosing a control law $u = \psi(x)$ which stabilizes the origin (i.e., regulates *x* to zero) while minimizing the quadratic cost function

$$J = \int_0^\infty x(t)^T Qx(t) + u(t)^T Ru(t)dt \tag{9}$$

where $Q = Q^T \geq 0$ and $R = R^T > 0$. The term "linear-quadratic" refers to the linear system dynamics and the quadratic cost function.

The matrices Q and R are called the state and control penalty matrices, respectively. If the components of Q are chosen large relative to those of R, then deviations of x from zero will be penalized heavily relative to deviations of u from zero. On the other hand, if the components of R are large relative to those of Q, then control effort will be more costly and the state will not converge to zero as quickly.

A famous and somewhat surprising result due to Kalman is that the control law which minimizes J always takes the form $u=\Psi(x)=-Kx$. The optimal regulator for a LTI system with respect to the quadratic cost function above is always a linear control law. With this observation in mind, the closed-loop system takes the form

$$\dot{x} = (\mathbf{A} - \mathbf{B}K)x \tag{10}$$

and the cost function J takes the form

$$J = \int_0^\infty x(t)^T Qx(t) + (-Kx(t))^T R(-Kx(t))dt \tag{11}$$

$$J = \int_0^\infty x(t)^T (Q + K^T RK)x(t)dt \tag{12}$$

Assuming that the closed-loop system is internally stable, which is a fundamental requirement for any feedback controller, the following theorem allows the computation value of the cost function for a given control gain matrix K.

Input Shaping Control Schemes:

Input shaping technique is a feed-forward control technique that involves convolving a desired command with a sequence of impulses known as input shaper. The shaped command that results from the convolution is then used to drive the system. Design objectives are to determine the amplitude and time locations of the impulses, so that the shaped command reduces the detrimental effects of system flexibility. These parameters are obtained from the natural frequencies and damping ratios of the system. Thus, sway reduction of a gantry crane system can be achieved with the input shaping technique. Figure 2 illustrates the input shaping process. Several techniques have been investigated to obtain an efficient input shaper for a particular system. A brief description and derivation of the control technique is presented in this section.

Generally, a vibratory system of any order can be modelled as a superposition of second order systems each with a transfer function

$$G(s) = \frac{\omega^2}{s^2 + 2\zeta\omega s + \omega^2} \tag{13}$$

where ω is the natural frequency of the vibratory system and ζ is the damping ratio of the system. Thus, the response of the system in time domain can be obtained as

$$y(t) = \frac{A\omega}{\sqrt{1-\zeta^2}} \exp^{-\zeta\omega(t-t_0)} \sin\left(\omega\sqrt{1-\zeta^2}(t-t_0)\right) \tag{14}$$

where A and t_0 are the amplitude and the time location of the impulse respectively. The response to a sequence of impulses can be obtained by superposition of the impulse responses. Thus, for N impulses, with $\omega_d = \omega\left(\sqrt{1-\zeta^2}\right)$ the impulse response can be expressed as

$$y(t) = M \sin\left(\omega_d t + \beta\right) \tag{15}$$

where

$$M = \sqrt{\left(\sum_{i=1}^{N} B_i \cos\phi_i\right)^2 + \left(\sum_{i=1}^{N} B_i \sin\phi_i\right)^2}$$, $B_i = \frac{A_i\omega}{\sqrt{1-\zeta^2}} \exp^{-\zeta\omega(t-t_0)}$, $\phi_i = \omega_d t_i$ and A_i and t_i are the amplitudes and time locations of the impulses.

The residual single mode sway amplitude of the impulse response is obtained at the time of the last impulse, t_N as

$$V = \sqrt{V_1^2 + V_2^2} \tag{16}$$

where

$$V_1 = \sum_{i=1}^{N} \frac{A_i \omega_n}{\sqrt{1-\zeta^2}} \exp^{-\zeta\omega_n(t_N - t_i)} \cos(\omega_d t_i) \quad ; \quad V_2 = \sum_{i=1}^{N} \frac{A_i \omega_n}{\sqrt{1-\zeta^2}} \exp^{-\zeta\omega_n(t_N - t_i)} \sin(\omega_d t_i)$$

To achieve zero sway after the last impulse, it is required that both V_1 and V_2 in Equation (16) are independently zero. This is known as the zero residual sway constraints. In order to ensure that the shaped command input produces the same rigid body motion as the unshaped reference command, it is required that the sum of amplitudes of the impulses is unity. This yields the unity amplitude summation constraint as

$$\sum_{i=1}^{N} A_i = 1 \tag{17}$$

In order to avoid response delay, time optimality constraint is utilised. The first impulse is selected at time $t_1 = 0$ and the last impulse must be at the minimum, i.e. min (t_N). The robustness of the input shaper to errors in natural frequencies of the system can be increased by taking the derivatives of V_1 and V_2 to zero. Setting the derivatives to zero is equivalent to producing small changes in sway corresponding to the frequency changes. The level of robustness can further be increased by increasing the order of derivatives of V_1 and V_2 and set them to zero. Thus, the robustness constraints can be obtained as

$$\frac{d^i V_1}{d\omega_n^{\ i}} = 0 \quad ; \quad \frac{d^i V_2}{d\omega_n^{\ i}} = 0 \tag{18}$$

Both the positive and modified SNA input shapers are designed by considering the constraints equations. The following section will further discuss the design of the positive and modified SNA input shapers.

Positive Input Shaper:

The positive input shapers have been used in most input shaping schemes. The requirement of positive amplitude for the impulses is to avoid the problem of large amplitude impulses. In this case, each individual impulse must be less than one to satisfy the unity magnitude constraint. In order to increase the robustness of the input shaper to errors in natural frequencies, the positive ZSDD input shaper is designed by setting the second derivatives of V_1 and V_2 in Equation (16) to zero. Simplifying $d^2V_i / d\omega_n^2$ yields

$$\frac{d^2 V_1}{d\omega_n^{\ 2}} = \sum_{i=1}^{N} A_i t_i^2 e^{-\zeta\omega_n(t_N - t_i)} \sin(\omega_d t_i); \quad \frac{d^2 V_2}{d\omega_n^{\ 2}} = \sum_{i=1}^{N} A_i t_i^2 e^{-\zeta\omega_n(t_N - t_i)} \cos(\omega_d t_i) \tag{19}$$

The positive ZSDD input shaper, i.e. four-impulse sequence is obtained by setting Equations (16) and (17) to zero and solving with the other constraint equations. Hence, a four-impulse sequence can be obtained with the parameters as

$$t_1 = 0,\ t_2 = \frac{\pi}{\omega_d},\ t_3 = \frac{2\pi}{\omega_d},\ t_4 = \frac{3\pi}{\omega_d}$$

$$A_1 = \frac{1}{1+3K+3K^2+K^3}, \quad A_2 = \frac{3K}{1+3K+3K^2+K^3} \tag{20}$$

$$A_3 = \frac{3K^2}{1+3K+3K^2+K^3}, \quad A_4 = \frac{K^3}{1+3K+3K^2+K^3}$$

where

$$K = e^{-\zeta\pi / \sqrt{1-\zeta^2}}, \quad \omega_d = \omega_n \sqrt{1-\zeta^2}$$

ω_n and ζ representing the natural frequency and damping ratio respectively. For the impulses, t_j and A_j are the time location and amplitude of impulse j respectively.

Modified SNA Input Shapers:

Input shaping techniques based on positive input shaper have been proved to be able to reduce sway of a system. In order to achieve higher robustness, the duration of the shaper is increased and thus, increases the delay in the system response. By allowing the shaper to contain negative impulses, the shaper duration can be shortened, while satisfying the same robustness constraint.

To include negative impulses in a shaper requires the impulse amplitudes to switch between 1 and -1 as

$$A_i = (-1)^{i+1} \quad ; \quad i = 1, \dots \dots, n \tag{21}$$

The constraint in Equation (21) yields useful shapers as they can be used with a wide variety of inputs. For a UM negative ZS shaper, i.e. the magnitude of each impulse is $|1|$, the shaper duration is one-third of the vibration period of an undamped system, while the shaper duration for the positive shaper is half of the vibration period. However, the increase in the speed of system response achieved using the SNA input shapers is at the expense of some tradeoffs and penalties. The shapers containing negative impulses have tendency to excite unmodeled high modes and they are slightly less robust as compared to the positive shapers. Besides, negative input shapers require more actuator effort than the positive shapers due to high changes in the set-point command at each new impulse time location.

To overcome the disadvantages, a modified SNA input shaper is introduced, whose negative amplitudes can be set to any value at the centre between each normal impulse sequences. In this work, the previous SNA input shaper (Mohamed *et al.,* 2006) is modified by locating the negative amplitudes at the centre between each positive impulse sequences with even number of total impulses. This will result the shaper duration as one-fourth of the sway period of an undamped system as shown in Figure 4. The modified SNA-ZSDD shaper is proposed and applied in this work to enhance the robustness capability of the controller while increasing the speed of the system response. By considering the form of modified SNA-ZSDD shaper shown in Figure 3, the amplitude summation constraints equation can be obtained as

$$2a + 2c - 2b - 2d = 1 \tag{22}$$

The values of a, b, c and d can be set to any value that satisfy the constraint in (22). However, the suggested values of a, b, c and d are less than $|1|$ to avoid the increase of the actuator effort.

Implementation and Result:

In this section, the proposed control schemes are implemented and tested within the simulation environment of the gantry crane and the corresponding results are presented. In this work, positive ZSDD and modified SNA-ZSDD are investigated as the input shaping control schemes. The cart position of the gantry crane is required to follow a trajectory within the range of ±4 m as shown in Figure 4. System responses namely the cart position, cart velocity and sway angle of the hoisting rope are observed. To investigate the sway of the system in the frequency domain, power spectral density (PSD) of the response at the sway angle is obtained. The performances of the hybrid controllers are assessed in terms of input tracking and sway suppression in comparison to the LQR control. Moreover, robustness of the controllers to variations in sway frequencies is also investigated. In this case, 30% error tolerance in sway frequencies is considered.

LQR control:

In this investigation, the tracking performance of the LQR control applied to the gantry crane system was investigated by obtaining the value of vector K and $\bar{N}$ which determines the feedback control law and for elimination of steady state error capability respectively. Using the lqr function in the Matlab, both vector K and $\bar{N}$ were set as

$$K = \begin{bmatrix} 700 & 428.3885 & 3.8267 & 1.4066 \end{bmatrix} \quad \text{and} \quad \bar{N} = \begin{bmatrix} 700 \end{bmatrix}$$

The responses of the gantry crane system to the unshaped trajectory reference input were analyzed in time-domain and frequency domain (spectral density) as shown in Figure 5. These results were considered as the system response to the unshaped input under tracking capability and will be used to evaluate the performance of the input shaping techniques. Simulation results with LQR controller have shown that the steady-state cart position trajectory of +4 m for the gantry crane was achieved within the rise and settling times and overshoot of 1.372 s, 2.403 s and 0.20 % respectively. It is noted that the cart reaches the required position from +4 m to -4 m within 3 s, with little overshoot.

However, a noticeable amount of sway angle occurs during movement of the cart. It is noted from the sway angle response with a maximum residual of ±1.4 rad. Moreover, from the PSD of the sway angle response the sway frequencies are dominated by the first three modes, which are obtained as 0.3925 Hz, 1.177 Hz and 2.06 Hz with magnitude of 33.02 dB, -9.929 dB and -22.86 dB respectively. The closed loop parameters with the LQR control will subsequently be used to design and evaluate the performance of hybrid controllers with positive ZSDD and SNA-ZSDD shapers.

Hybrid Control:

Figure 6 shows a block diagram of the proposed hybrid control scheme where the LQR controller is combined with the input shaping control schemes. The positive ZSDD and modified SNA-ZSDD shapers were designed based on the dynamic behaviour of the closed-loop system obtained using only the LQR control. As demonstrated in the previous section, the natural frequencies of the sway angle were 0.3925 Hz, 1.177 Hz and 2.06 Hz for the first three sway modes. With exact natural frequencies, the time locations and amplitudes of the impulses for positive ZSDD shaper were obtained by solving Equation (20). Moreover, the amplitudes of the modified SNA-ZSDD shaper were deduced as [0.3 -0.1 0.5 -0.2 0.5 -0.2 0.3 -0.1] and the time locations of the impulses were chosen at the half of the time locations of positive ZSDD shaper as shown in Figure 3. For evaluation of robustness, input shapers with erroneous natural frequencies were also evaluated. With 30% error in natural frequency, the system sways were considered at 0.5103 Hz, 1.5301 Hz and 2.678 Hz for the three modes of sway. Similarly, the amplitudes and time locations of the input shapers with 30% erroneous natural frequencies for both the positive and modified SNA-ZSDD shapers were calculated.

For digital implementation of the input shaper, locations of the impulses were selected at the nearest sampling time. The developed input shaper was then used to pre-process the input reference shown in Figure 4. Figure 7 shows the shaped inputs using both the positive and modified SNA-ZSDD shapers with exact natural frequencies. It is noted that the shaped input with the modified SNA shaper is not as smooth as compared to the positive shaper. This is due to higher number of switching of the actuator.

Figure 8 shows the system responses of the gantry crane using the hybrid controllers with exact natural frequencies. Table 1 summarises the levels of sway reduction of the system responses at the first three modes in comparison to the LQR control. It is noted that the proposed hybrid controllers are capable of reducing the system sway while maintaining the input tracking performance of the cart position. Similar cart position and cart velocity responses were observed as compared to the LQR controller. Moreover, a significant amount of sway reduction was demonstrated at the sway angle of the hoisting rope with both control schemes. With the positive ZSDD and modified SNA-ZSDD shapers, the maximum sway angles were obtained at ±0.16 rad and ±0.20 rad respectively. These are nine-fold and seven-fold improvements as compared to LQR control. This is also evidenced in the PSD of the sway angle residual that shows lower magnitudes at the resonance modes. The corresponding rise time, setting time and overshoot of the cart response using LQR control with positive and modified SNA ZSDD shapers with exact natural frequencies is depicted in Table 1. The simulation results show that the cart position reaches the required trajectory position of +4 m within the settling times of 6.285 s and 5.573 s with positive ZSDD and modified SNA-ZSDD respectively. It is noted with the feed-forward controller, a slower settling time as compared to the LQR controller was achieved.

To examine the robustness of the hybrid controllers, the shapers with 30% error in sway frequencies were designed and implemented to the gantry crane system. Figure 9 shows the response of the gantry crane with the hybrid controllers with erroneous natural frequencies. Table 1 summarises the levels of sway reduction with erroneous natural frequencies in comparison to the LQR control. The time response specifications of the cart position with error in natural frequencies are also summarised in Table 1. Similar to the case with exact frequencies, the proposed hybrid controllers are capable of reducing the system sway while maintaining the input tracking performance of the cart position. Moreover, the sways of the system were considerable reduced as compared to the response with LQR controller. However, the level of sway reduction is slightly less than the case with exact natural frequencies.

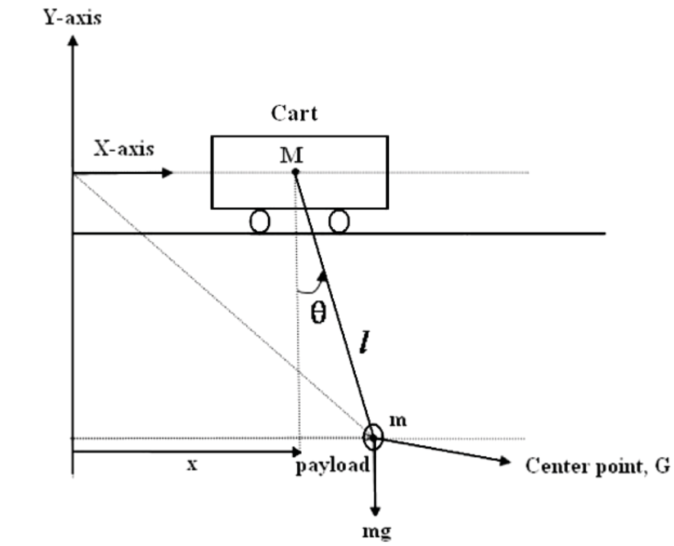

Fig. 1: Description of the gantry crane system.

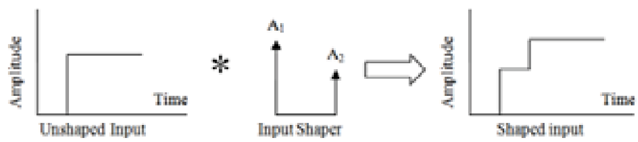

Fig. 2: Illustration of input shaping technique.

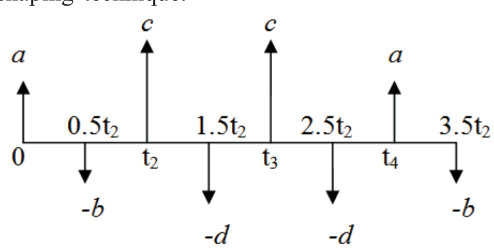

Fig. 3: Modified SNA-ZSDD shaper.

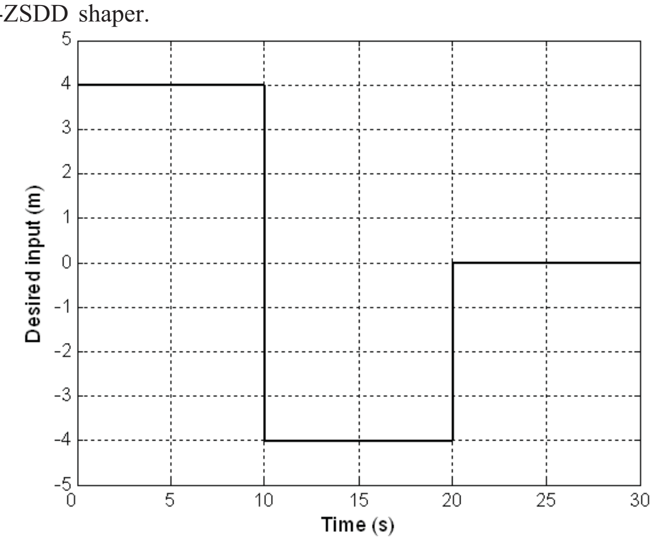

Fig. 4: The trajectory reference input.

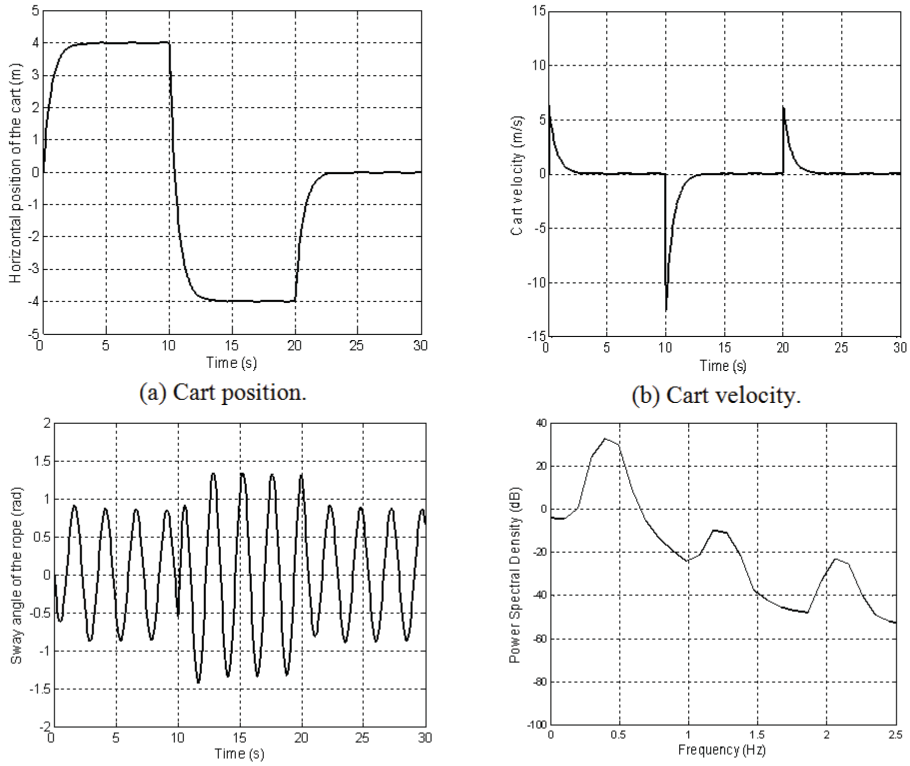

(a) Cart position. (b) Cart velocity.

(c) Sway angle. (d) PSD of sway angle.

Fig. 5: Response of the gantry crane with LQR controller.

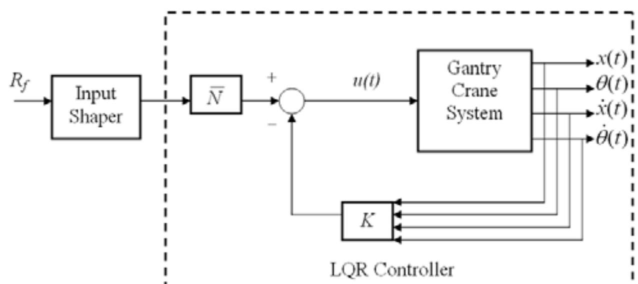

Fig. 6: Block diagram of the hybrid control schemes configuration.

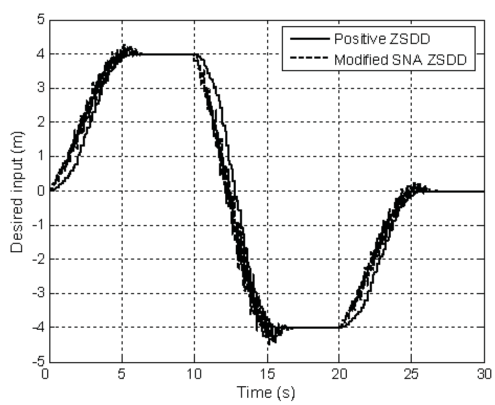

Fig. 7: Shaped inputs with exact natural frequencies using positive ZSDD and modified SNA-ZSDD shapers.

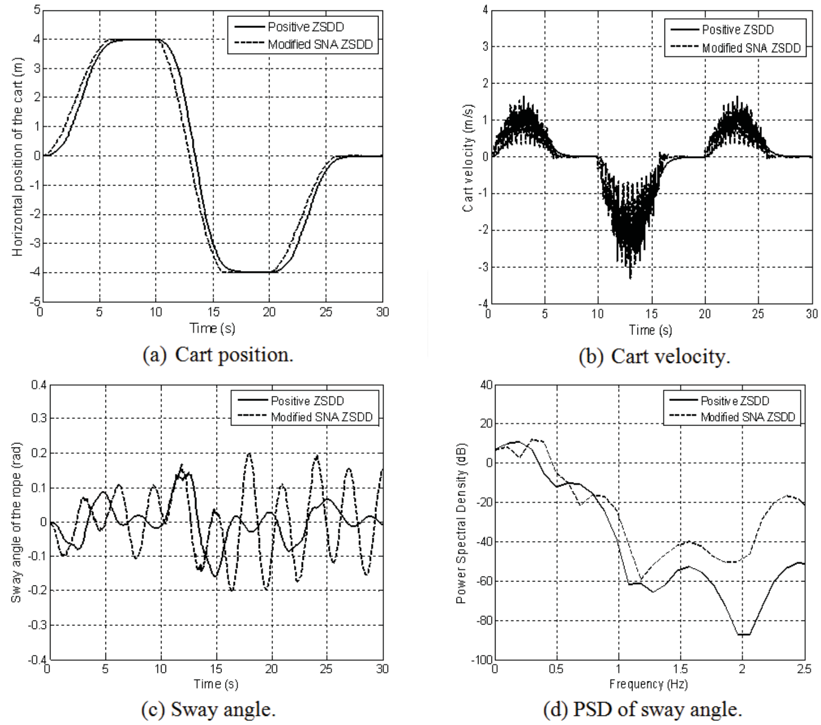

(a) Cart position. (b) Cart velocity.

(c) Sway angle. (d) PSD of sway angle.

Fig. 8: Response of the gantry crane with hybrid controllers with exact natural frequencies.

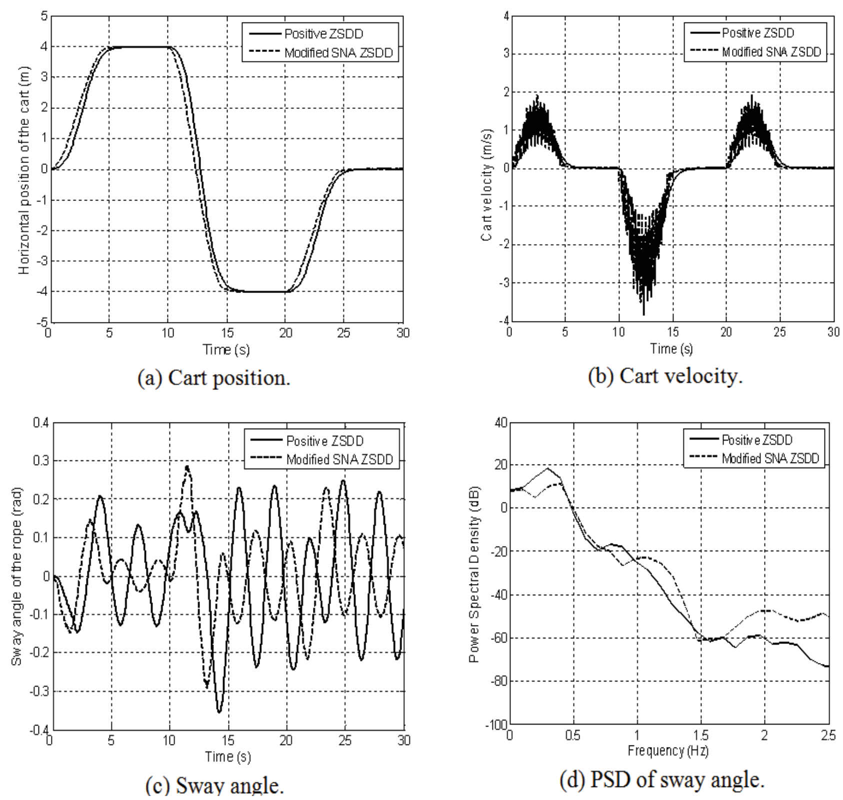

(a) Cart position. (b) Cart velocity.

(c) Sway angle. (d) PSD of sway angle.

Fig. 9: Response of the gantry crane with hybrid controllers with erroneous natural frequencies.

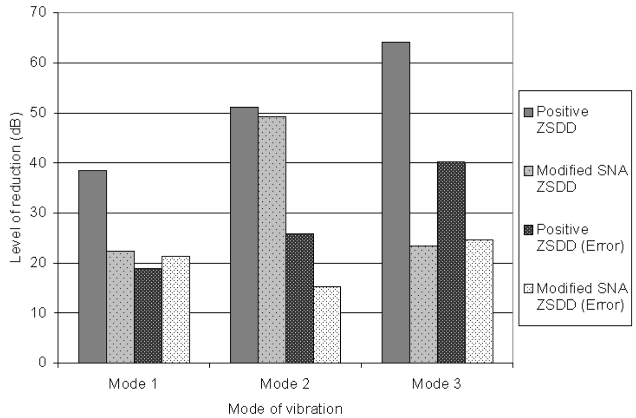

Fig. 10: Level of sway reduction with exact and erroneous natural frequencies with hybrid controllers.

Table 1: Level of sway angle reduction of the rope and specifications of the cart trajectory response for the hybrid control schemes

Frequency	Types of shaper (ZSDD)	Attenuation (dB) of sway angle of the rope			Specifications of cart trajectory response		
		Mode 1	Mode 2	Mode 3	Rise time (s)	Settling time (s)	Overshoot (%)
Exact	Positive	38.45	51.20	64.18	3.448	6.285	0.00
	Modified SNA	22.46	49.17	23.42	4.462	5.573	0.03
Error	Positive	18.97	25.91	40.17	2.787	5.241	0.00
	Modified SNA	21.39	15.31	24.71	2.995	4.621	0.03

The simulation results show that performance of the hybrid controller with positive ZSDD control scheme is better than SNA-ZSDD scheme in sway suppression of the gantry crane. This is further evidenced in Figure 10 that demonstrates the level of sway reduction of the gantry crane with the hybrid controllers as compared to the LQR controller. It is noted that higher sway reduction is achieved with positive ZSDD at the first, second and third resonance modes, which are the most dominant modes. Almost two-fold improvement in the sway reduction was observed as compared to SNA-ZSDD. Comparisons of the cart position responses show that the hybrid controller with SNA-ZSDD shaper is faster than the case using the positive ZSDD shaper. The result reveals that the speed of the system responses can be improved by using negative impulses input shaper.

Comparison of the results shown in Figure 10 reveals that both hybrid controllers with the positive and SNA input shapers can successfully handle errors in natural frequencies. Moreover, almost similar performance in sway reduction of the gantry crane was achieved with both control schemes. As positive ZSDD performs better than SNA-ZSDD with exact frequencies, the results demonstrate that, the modified SNA-ZSDD is capable of improving the robustness of the controller to uncertainty in sway frequencies. Comparisons of the cart position response with the hybrid controllers show a similar pattern as the case with exact natural frequencies. With the new proposed SNA shaper, it is shown that the robustness of the controller can be improved while increasing the speed of the response. The work thus developed and reported in this paper forms the basis of design and development of hybrid control schemes for input tracking and sway suppression of boom and 3-D gantry crane systems and can be extended to and adopted in practical applications.

Conclusion:

The development of hybrid control schemes based on LQR control with positive and negative input shapers for input tracking and sway suppression of a gantry crane has been presented. The proposed control schemes have been implemented and tested within simulation environment of an overhead gantry crane derived using the Euler-Lagrange formulation. The performances of the control schemes have been evaluated in terms of input tracking capability, level of sway reduction and robustness. Acceptable performance in input tracking control and sway suppression has been achieved with both control strategies. Moreover, a significant reduction in the system sways has been achieved with the hybrid controllers regardless of the polarities of the shapers. A comparative assessment of the hybrid control schemes has shown that the LQR control with positive ZSDD shaper provides higher level of sway reduction of the gantry crane as compared to the LQR with SNA-ZSDD shaper. By using the LQR control with modified SNA-ZSDD, robustness of the controller can be improved as similar level of robustness as positive ZSDD is achieved. Moreover, with SNA -ZSDD, the speed of the response is slightly increased at the expenses of decrease in the level of sway reduction.

REFERENCES

Auernig, J. and H. Troger, 1987. Time optimal control of overhead cranes with hoisting of the load. *Automatica*, 23(4): 437-447.

Belanger, N.M., 1995. Control Engineering: A Modern Approach, Saunders College Publishing.

Feddema, J.T., 1993. Digital Filter Control of Remotely Operated Flexible Robotic Structures. *American Control Conference*, San Francisco, CA, 3: 2710-2715.

Karnopp, B.H., F.E. Fisher and B.O. Yoon, 1992. A strategy for moving mass from one point to another. Journal of the Franklin Institute, 329: 881-892.

Kress, R.L., J.F. Jansen and M.W. Noakes, 1994. Experimental Implementation of a Robust Damped-Oscillation Control Algorithm on a Full Sized, Two-DOF, AC Induction Motor- Driven Crane. *5th ISRAM*, Maui, HA, pp: 585-92.

Manson, G.A., 1992. Time-optimal control of and overhead crane model. Optimal Control Applications & Methods, 3(2): 115-120.

Mohamed, Z., A.K. Chee, Mohd A.W.I. Hashim, M.O. Tokhi, S.H.M. Amin and R. Mamat, 2006. Techniques for vibration control of a flexible manipulator. *Robotica* 24: 499-511.

Noakes, M.W. and J.F. Jansen, 1992. Generalized Inputs for Damped-Vibration Control of Suspended Payloads. Robotics and Autonomous Systems, 10(2): 199-205.

Omar, H.M., 2003. Control of gantry and tower cranes. Ph.D. Thesis, M.S. Virginia Tech.

Ogata, K., 1997. *Modern Control Engineering*. Prentice-Hall International, Upper Saddle River, NJ.

Singer, N., W. Singhose and E. Kriikku, 1997. An Input Shaping Controller Enabling Cranes to Move Without Sway. ANS 7th Topical Meeting on Robotics and Remote Systems, Augusta, GA.

Singhose, W., N.C. Singer and W.P. Seering, 1994. Design and implementation of time-optimal negative input shapers. *Proceedings of International Mechanical Engineering Congress and Exposition*, Chicago, pp: 151-157.

Singhose, W. and B.W. Mills, 1999. Command generation using specified-negative-amplitude input shapers. *Proceedings of the American Control Conference*, San Diego, California, pp: 61-65.

Singhose, W.E., L.J. Porter and W. Seering, 1997. Input shaped of a planar gantry crane with hoisting. Proc. of the American Control Conference, pp: 97-100.

Teo, C.L., C.J. Ong and M. Xu, 1998. Pulse input sequences for residual vibration reduction. Journal of Sound and Vibration, 211(2): 157-177.

Wahyudi and J. Jalani, 2005. Design and implementation of fuzzy logic controller for an intelligent gantry crane system. Proceedings of the 2nd International Conference on Mechatronics, pp: 345- 351.